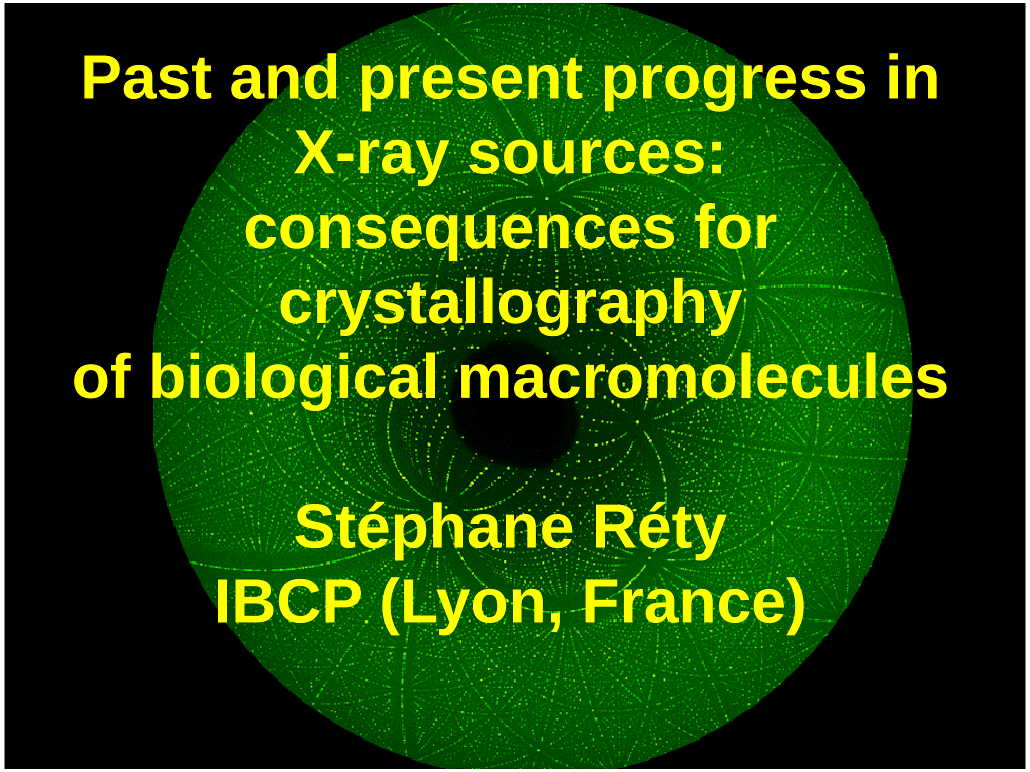

Past and present progress in X-ray sources: consequences for crystallography of biological macromolecules

Stéphane Réty
IBCP (Lyon, France)

1895: First X-rays

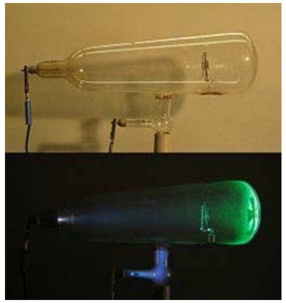

Crookes tubes are cold cathode tubes: from a few kilovolts to about 100 kilovolts is applied between the electrodes.
The Crookes tubes require a pressure from about 10^{-6} to 5×10^{-8} atmosphere.

German physicist Wilhelm Röntgen, credited as the discoverer of X-rays in 1895

Wilhelm Röntgen's first "medical" X-ray, of his wife's hand, taken on 22 December 1895 and presented to Ludwig Zehnder of the Physik Institut, University of Freiburg, on 1 January 1896

Use of X-ray to study the structure of matter

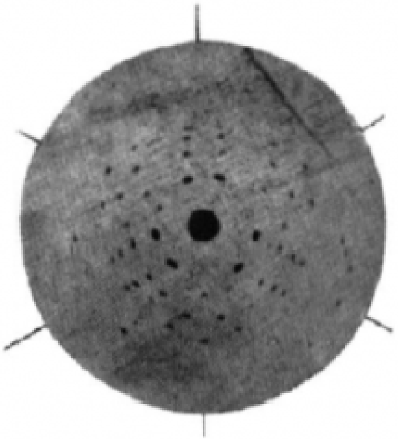

First published diffraction pattern of a crystal of Zinc blend obtained by W. Friedrich, P. Knipping and M. Laue (1912). The 3-fold symmetry of the pattern is a reflection of the symmetrical arrangement of the atoms inside the crystal.

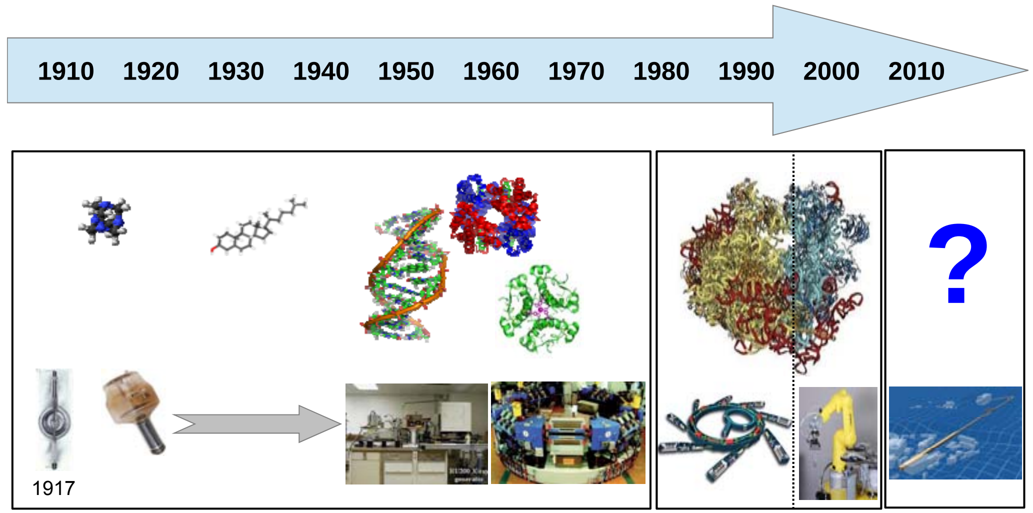

A X-ray diffraction experiment setup

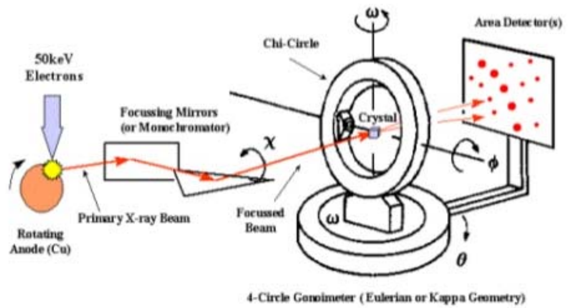

Source
- Flux of photons
- Brilliance : radiated power per unit area and per unit solid angle at the source

Optics
- Focussing mirros
- Monochromators

Detector
1.X-ray light is quantized (photons)
2. In order to detect you have to transfer energy from the particle to the detector
3. The energy absorbed is transfered into an electric signal and then into a number (digitized)

Detector readout must be of the same order as exposure time

The Detector Challenge:

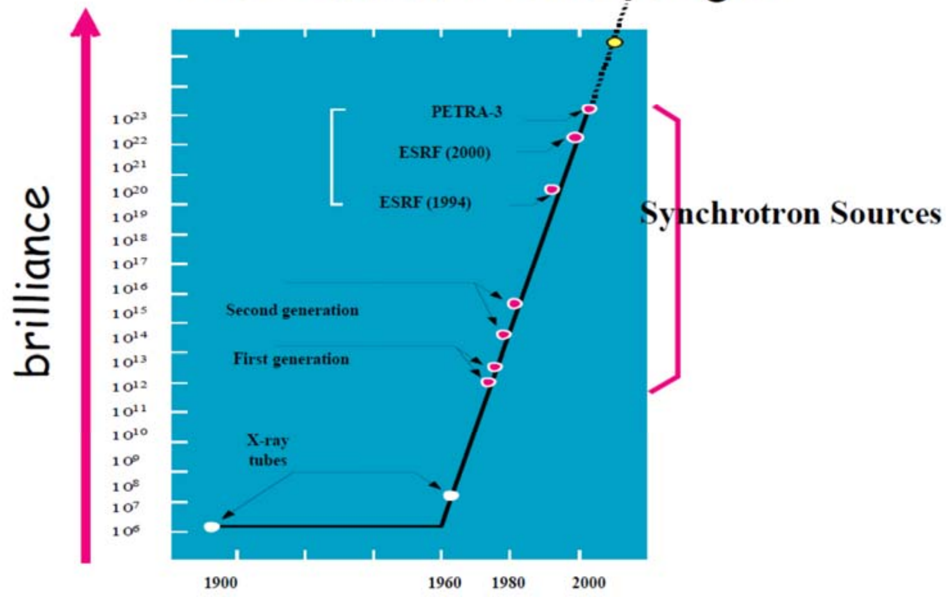

Some general detector parameters

- **QE** = quantum efficiency = fraction of incoming photons detected (<1.0). You want this to be as high as possible.
- **DQE** = detective quantum efficiency =

$$\frac{(signal/noise)_{out}}{(signal/noise)_{in}} \leq 1.0$$

You can never increase signal, nor decrease noise! So signal to noise will always degrade in the detector. (NB: **signal to noise is the most important parameter** when you measure something!)

- **Gain** = relation between your signal strength (V, A, ADU) and the number of photons.

1895-...: sealed tubes / rotating anodes
1-2nd generation synchrotrons

X-ray sources
Films / IP

Capillaries

Isomorphous replacement

Lab sources

Bremsstrahlung (braking radiation) ***Characteristic lines***
(source: nobelprize.org)

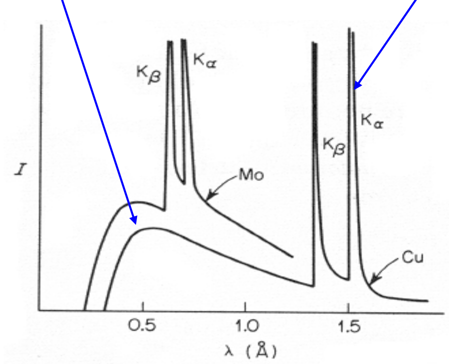

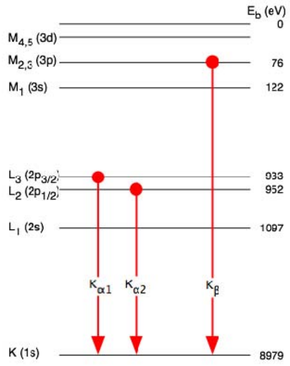

Lab sources

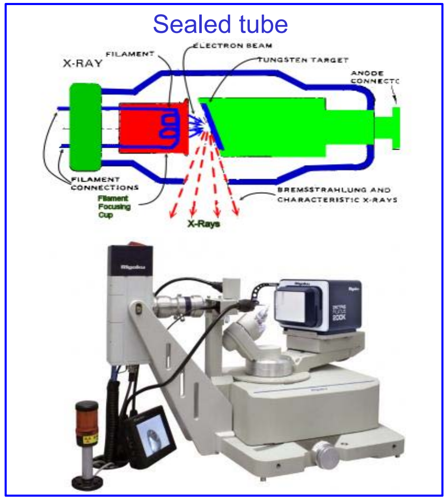

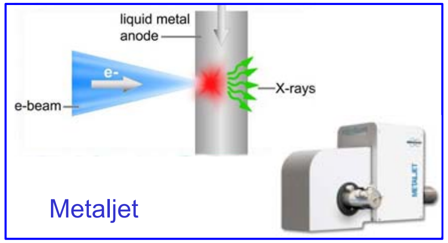

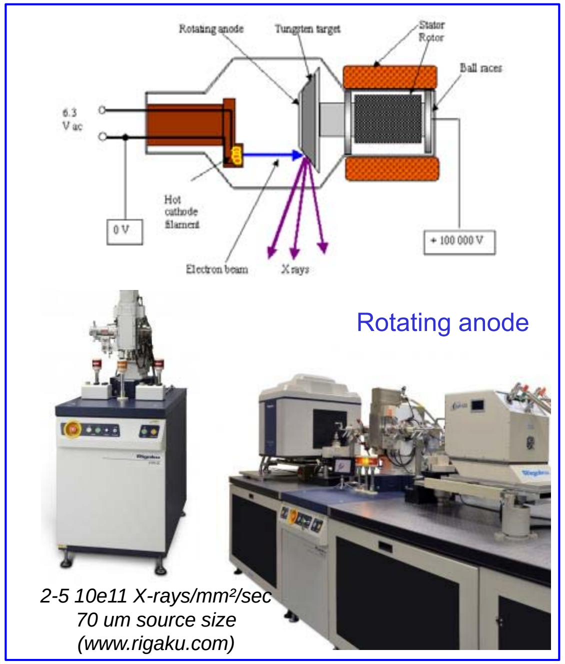

Synchroton generations

1st generation synchrotron: parasitic operation (50s to 70s)
ACO, DORIS, SPEARS...

ACO (www.media-paris-saclay.fr)

2nd generation synchrotron: dedicated to SR (80s)
SRS, DORIS, NSLS, LURE...

DORIS (http://www.desy.de)

3rd generation synchrotron: ID with high brightness, low emittance
ESRF, ALS,...

Synchrotron components

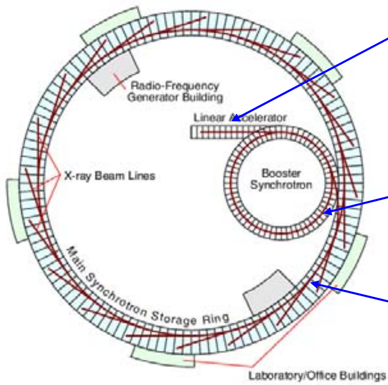

(http://pd.chem.ucl.ac.uk/pdnn/inst2/work.htm)

Linac
Electron beam generation
First beam acceleration

Booster
Acceleration to nominal energy

Storage ring
Beam storage for SR use

$$\gamma = \frac{1}{\sqrt{1-\frac{v^2}{c^2}}}$$

$$E_e = \gamma m c^2$$

Synchrotron components

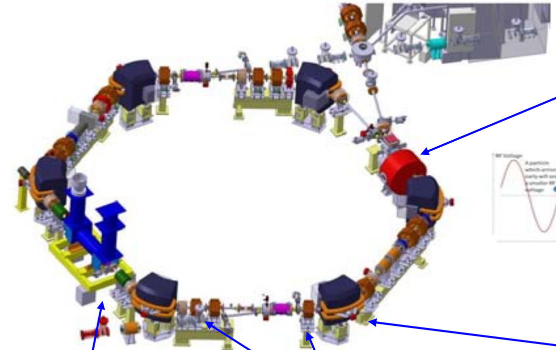

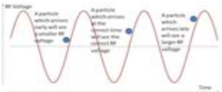

RF cavity
electron beam acceleration
(www.synchrotron-soleil.fr)

Dipole
for electron beam deviation
(www.synchrotron-soleil.fr)

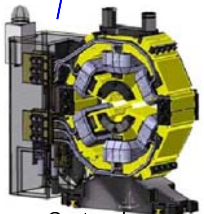

Sextupole
for electron beam stability
(www.synchrotron-soleil.fr)

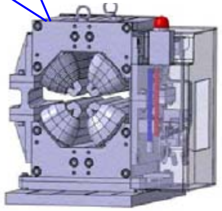

Quadripole
for electron beam focusing
(www.synchrotron-soleil.fr)

The multipole magnets refocus the beam after each deflection section, as deflection sections have a defocusing effect.

2[nd] generation synchrotrons

Bending magnet
A single magnetic dipole

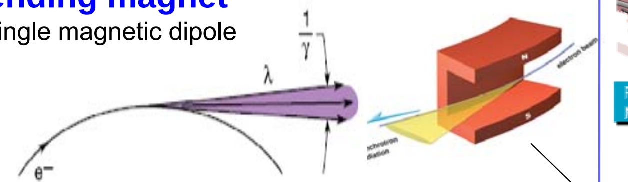

Wiggler
A series of magnetic dipoles
Large e- trajectory extension

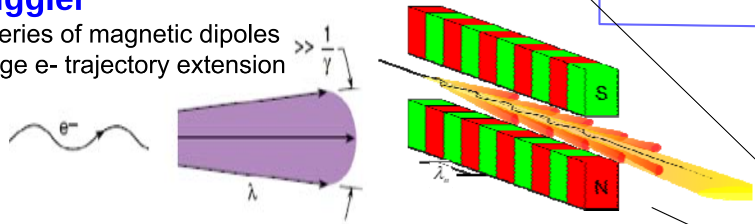

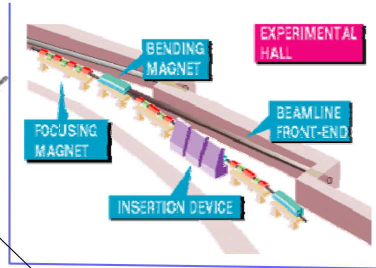

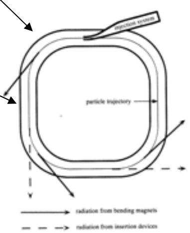

Brown et al. Nuclear Instruments and Methods, Volume 208, 1983, 65-77

Weissenberg method

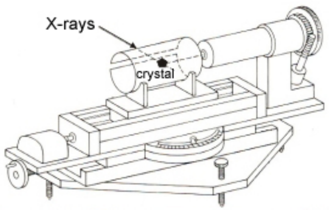

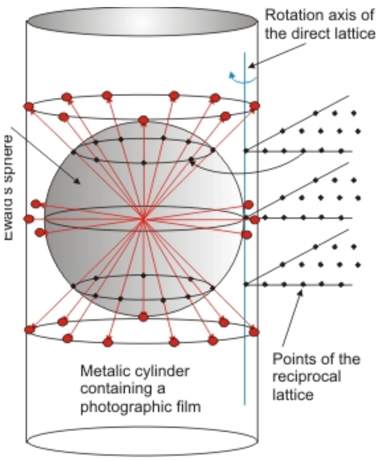

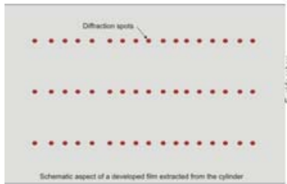

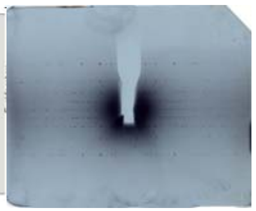

Precession method

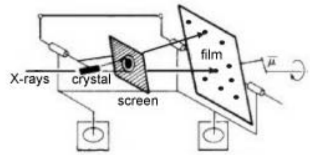

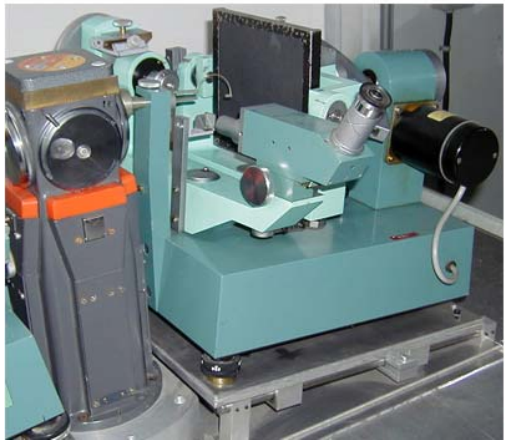

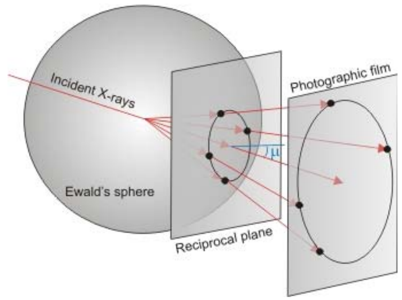

Oscillation method

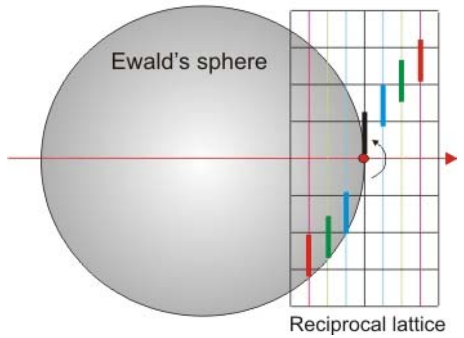

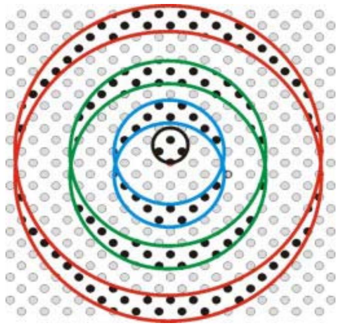

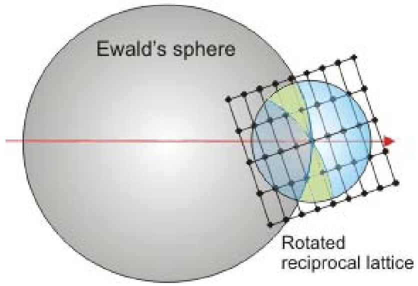

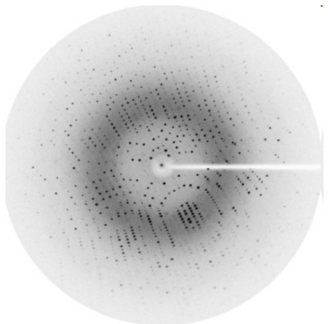

From photographic films to modern area detector

Counting versus Integrating

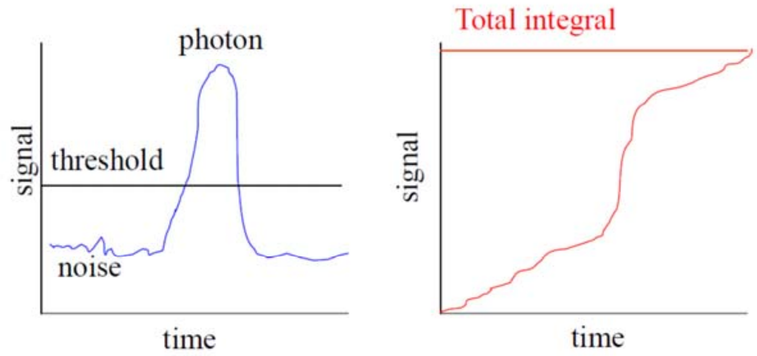

Low noise **Fast**

A multi-wire chamber at LURE
(1974-1992)

1st MAD structure!

LURE:
R. Kahn, R. Bosshard,
A.Bahri, G. Bricogne,
A. Bentley, R. Fourme
CERN:
R. Bouclier, R. Million
J.C. Santiard, G. Charpak

Multi-wire chamber

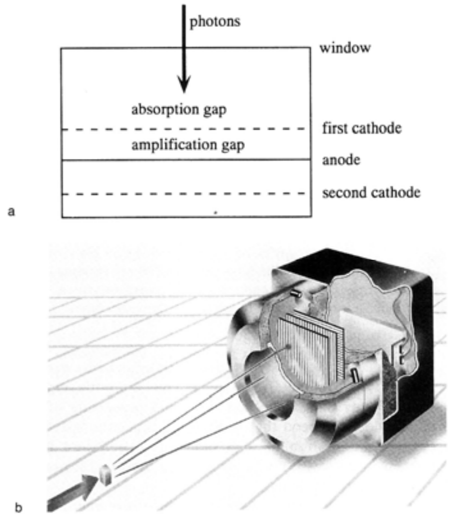

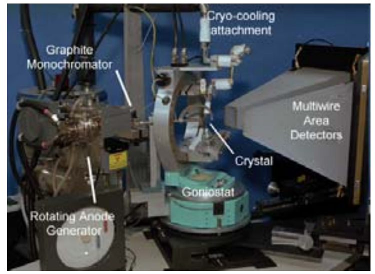

Xuong-Hamlin multiwire detector

Image Plate

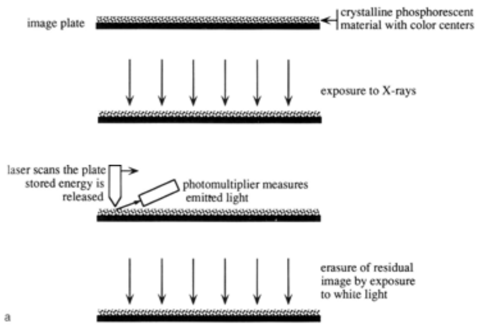

Upon exposure to X-ray:
Storage of the signal in the phosphor plate over a prolonged period,

Upon readout:
Photostimulated luminescence (PSL) releases the stored energy within the phosphor by stimulation with visible light, to produce a luminescent signal.

Exposure: 5 - 60 min
Readout: 5 min

Samples in capillaries

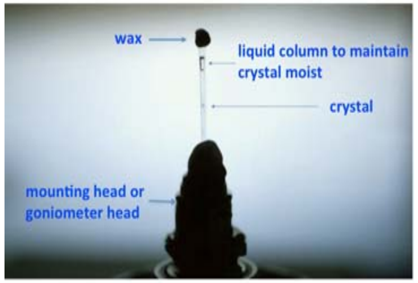

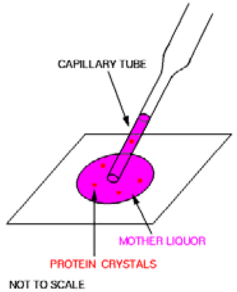

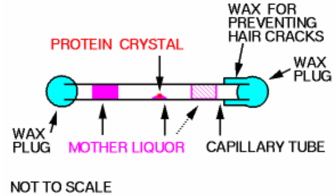

(www.mitegen.com/products/micrort/micrort.shtml)

1959: First protein structures

In 1953 **Max Perutz** showed that diffracted X-rays could be phased by comparing the patterns with and without heavy atoms attached. In 1959 he determined the structure of hemoglobin

Max Perutz and **John Kendrew** shared the 1962 Nobel Prize for Chemistry for the structures of hemoglobin.

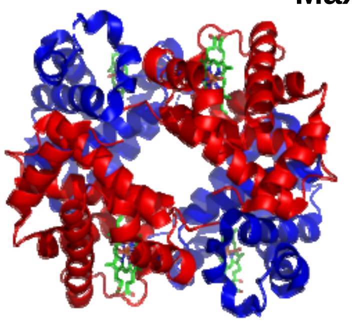

1969, **Dorothy Crowfoot Hodgkin** solved the 3D structure of insulin, on which she worked for over thirty years!!

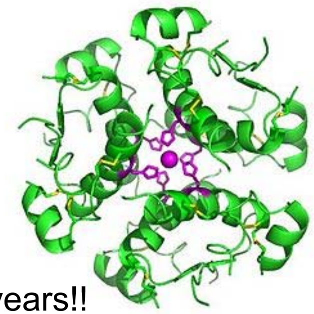

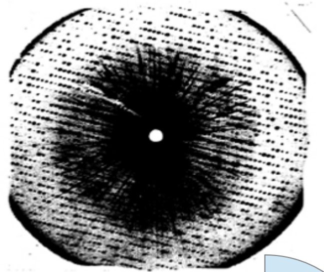

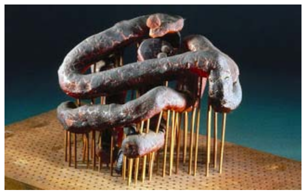

Myoglobin (1957)

Haemoglobin model 1957

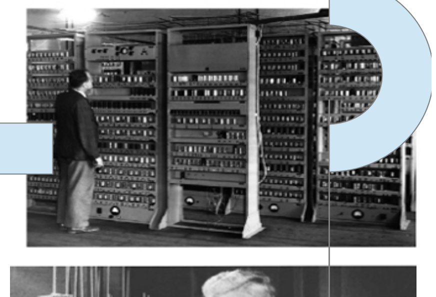

To analyse the 25,000 reflections of haemoglobin data, Perutz and Kendrew used the EDSAC I computer introduced in 1949

1990s: 3rd generation synchrotrons

X-ray sources
CCD detectors / HPD detectors

Freezing

Anomalous diffraction

3rd generation synchrotrons

ESRF (844m)

SOLEIL (354m)

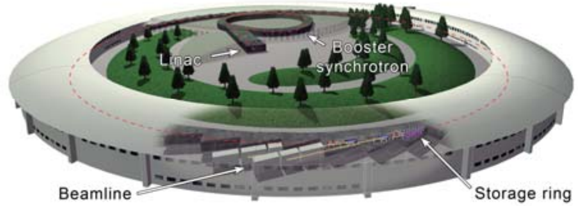

Third generation synchrotron facilities

ESRF	6	GeV	France
ALS	1.9	GeV	USA
APS	7	GeV	USA
BESSY II	1.7	GeV	Germany
ELETTRA	2.0	GeV	Italy
SPring-8	8	GeV	Japan
MAX II	1.5	GeV	Sweden
SLS	2.4	GeV	Switzerland
PLS	2	GeV	Korea
SRRC	1.4	GeV	Taiwan
SSRL	3	GeV	USA
CLS	2.9	GeV	Canada
Soleil	2.5	GeV	France
Diamond	3	GeV	UK
Australian Light Source	3	GeV	Australia
Alba	2	GeV	Barcelona
SSRF	3	GeV	Shanghai

3rd generation synchrotrons

Bending magnet

A single magnetic dipole

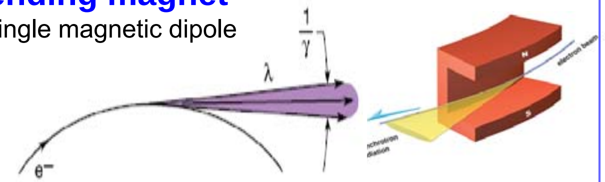

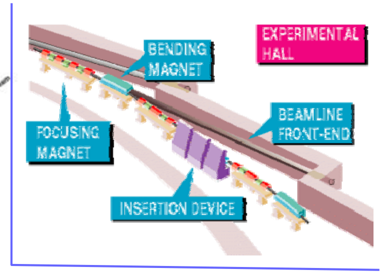

Wiggler

A series of magnetic dipoles $\gg \frac{1}{\gamma}$

Large e- trajectory extension

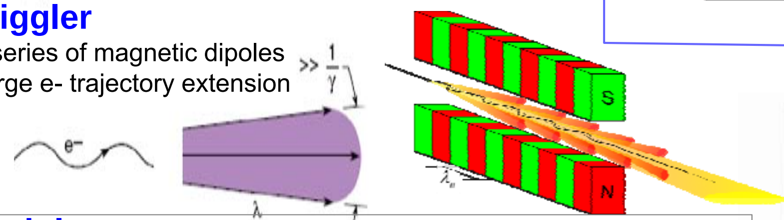

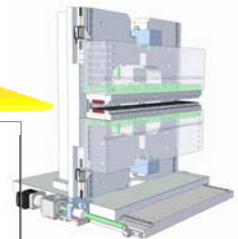

Undulator

A series of magnetic dipoles

Small e- trajectory extension $\frac{1}{\gamma\sqrt{N}}$

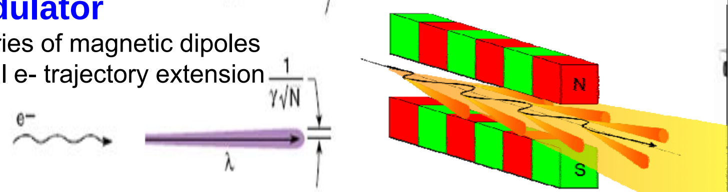

Brown et al. Nuclear Instruments and Methods, Volume 208, 1983, 65-77

Wiggler *vs* undulator

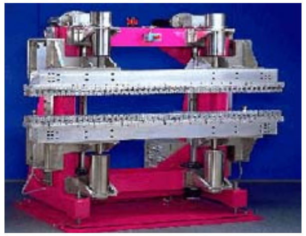

Wiggler

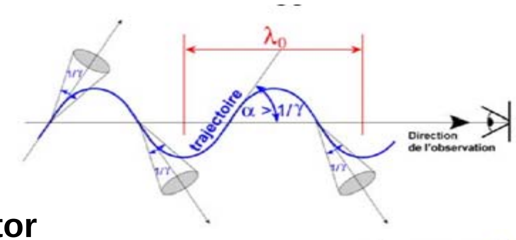

Undulator

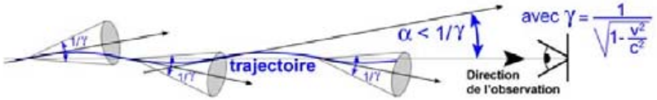

α : angular extension of the e- traj.

γ : emission cone aperture

In an undulator: $\alpha < 1/\gamma$

=> emission in presence of the beam

=> constructive interferences

=> spectral lines (brightness in N^2)

=> beam divergence in N$^{-1/2}$

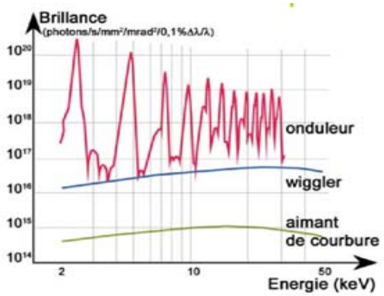

(www.synchrotron-soleil.fr/images/File/RessourcesPedagogiques/Documentation/Machine-FicheEnseignant.pdf)

3rd generation synchrotrons

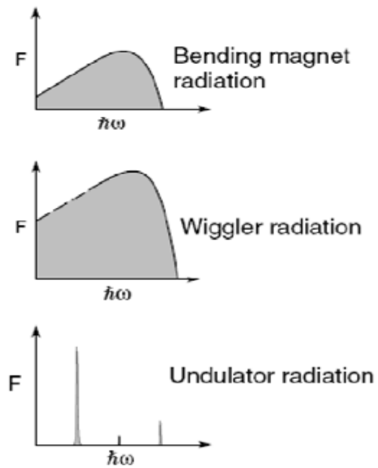

Jim Clarke, ASTeC, SRS

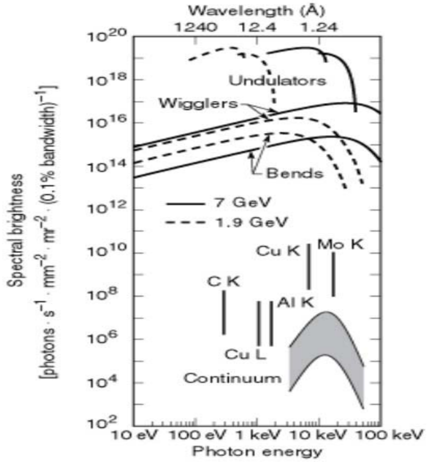

http://xdb.lbl.gov/Section2/Sec_2-1.html

					Bending magnet		Wiggler		Undulator	
Ring	Energy (GeV)	ρ (m)	I_b (mA)	P_{total} (kW)	$dP/d\theta$ (W/mrad)	$dP/d\Omega$ (W/mrad^2)	$dP/d\theta$ (W/mrad)	$dP/d\Omega$ (W/mrad^2)	$dP/d\theta$ (W/mrad)	$dP/d\Omega$ (W/mrad^2)
SRS (2nd generation)	2	5.56	200	50.9	8.1	20.8	4.0	0.6	1.0	2.2
DIAMOND	3	7.15	300	300.7	47.9	184.4	13.7	4.9	3.5	16.8
ESRF	6	25.0	200	916.5	145.9	1124.0	36.4	52.5	9.3	179.1

What are the relative merits?

Bending magnet radiation	Wiggler radiation	Undulator radiation
• Broad spectrum	• Higher photon energies	• Brighter radiation
• Good photon flux	• More photon flux	• Smaller spot size
• No heat load	• Expensive magnet structure	• Partial coherence
• Less expensive	• Expensive cooled optics	• Expensive
• Easier access	• Less access	• Less access

Cryo-cooling

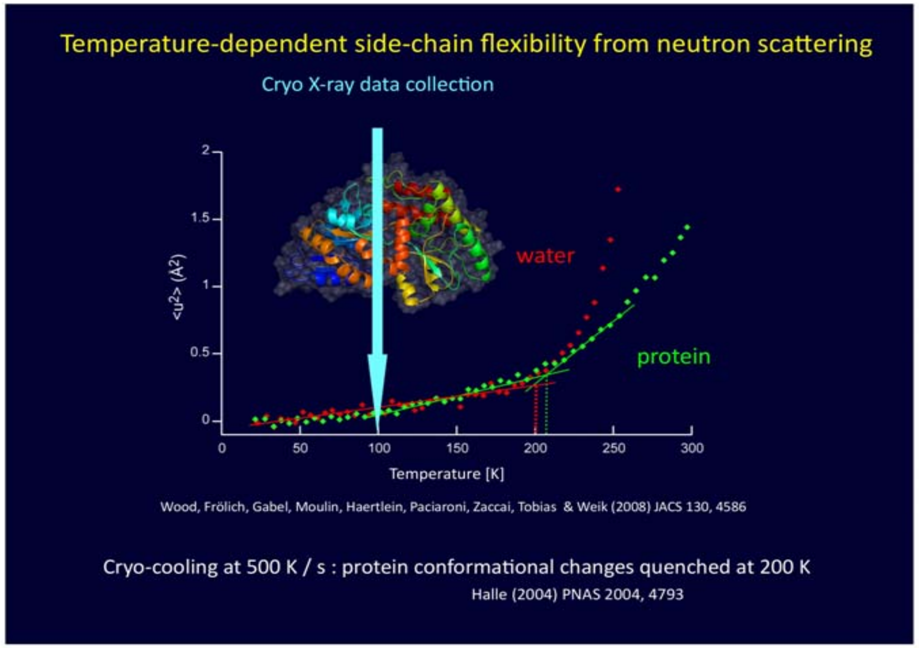

M. Weik, ESRF Users Meeting, 2014

Crystal flash-freezing

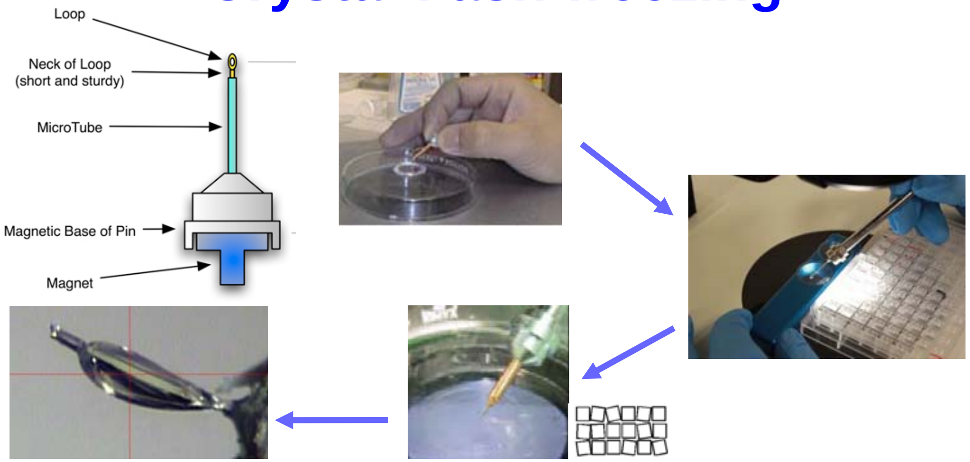

Possible improvements:
Optimized cryo-protectant
Absence of liquid (Pellegrini et al., Acta Cryst. (2011). D67, 902-6)
High speed freezing (Warkentin et al., J Appl Cryst. (2006) 39, 805–11)
Freezing in propane, etc...

Crystal flash-freezing
Last improvements

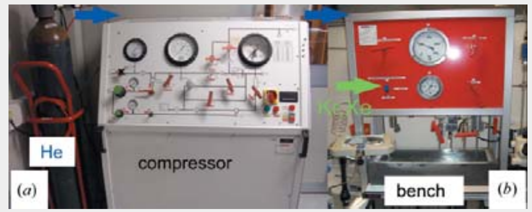

P. Carpentier, ESRF

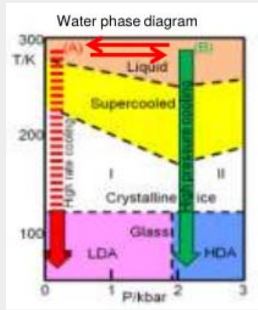

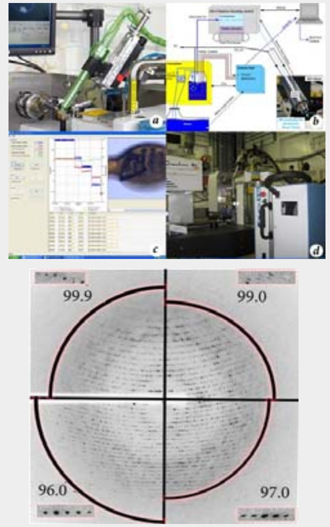

(Bowler et al., Cryst. Growth Des., (2015) 15, 1043−1055)

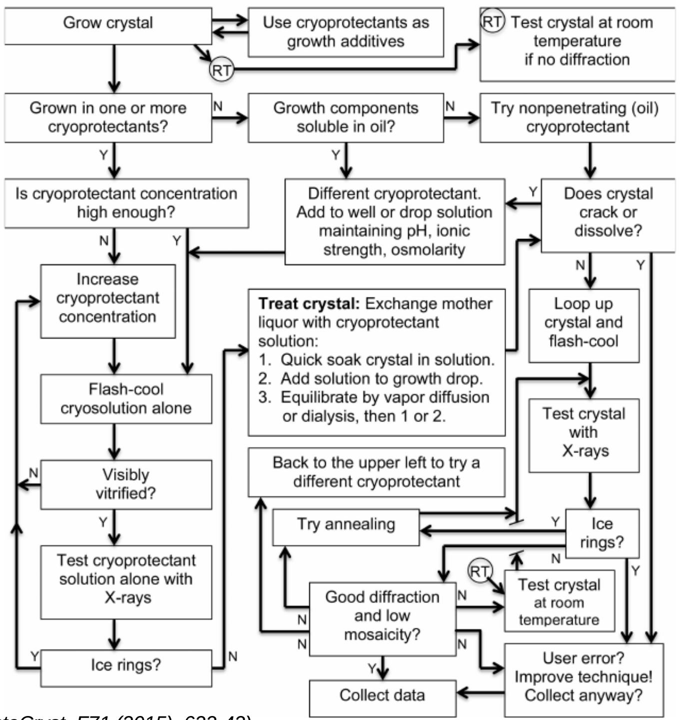

(J.W. Pflugrath, ActaCryst. F71 (2015), 622-42)

The anomalous signal

$$F(h) = \Sigma_j\, f_j \cdot \exp(2\pi i h \bullet r_j)$$
$$f_j = f^\circ_j(\theta) + f'_j(\lambda) + i \cdot f''_j(\lambda)$$

Anomalous correction f″ is proportional to absorption and fluorescence and f′ is its derivative

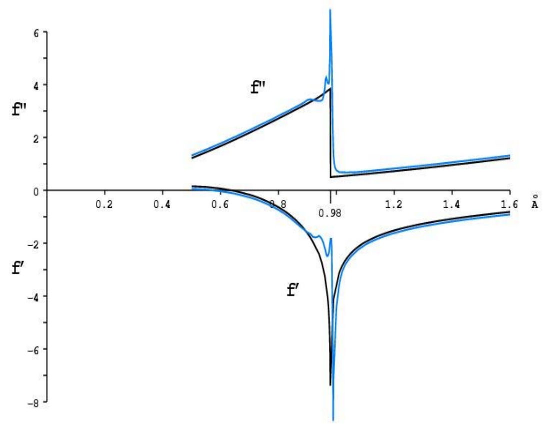

CCD detectors

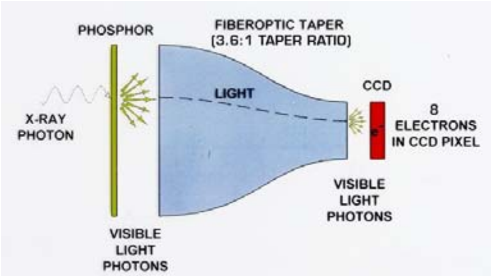

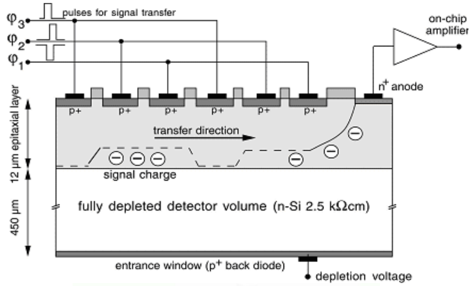

CCD = Charge Coupled Devices

- Very thin silicon layer that transfers photons into electrons ➔ not good for X-rays ➔ use intermediate scintillator/phosphor.
- Storage wells that store generated charge; including thermally induced charge = dark current ➔ fast but noisy
- Readout of signal through one readout node; transfer charge from one pixel to the next towards readout node ➔ long readout times
- Small pixels: 10 – 30 micrometer.
- Commercial product for large market ➔ perfect

Readout time compatible with synchrotron exposure time + high dynamic

Hybrid Pixel Area Detectors

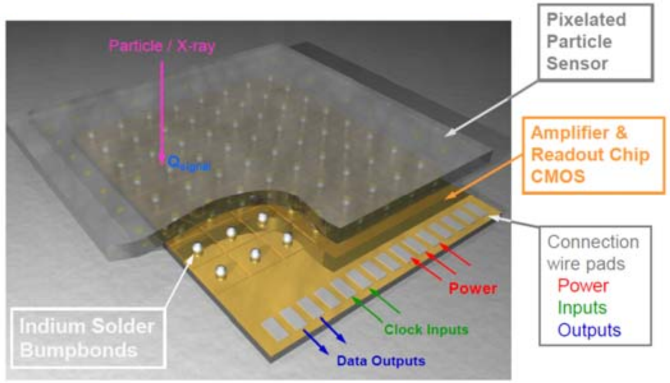

Particle / X-ray → Signal Charge → Electr. Amplifier → Readout → Digital Data

Short readout time
→ shutterless mode
→ fine slicing

Direct detection of photons in the sensor (no need for a scintillator for conversion to visible light photons).

Pflugrath, J. W. (1999). The finer things in X-ray diffraction data collection, *Acta Cryst. D* **55**, 1718-1725.

Pilatus 6M

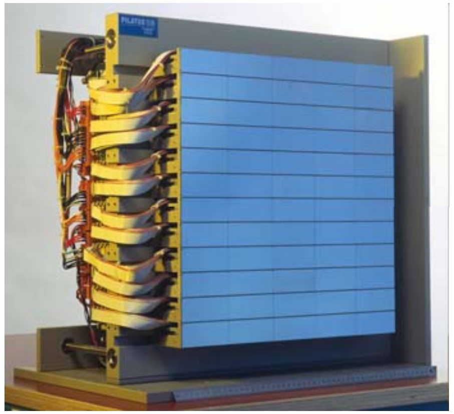

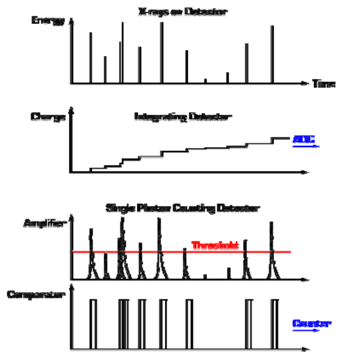

	Integrating Detector	PILATUS Detector
Principle	Charge is accumulated and then converted.	X-ray is counted above certain threshold.
Count Rate Dynamic Range	Unlimited	Limited to ~1.5 MHz/pixel/s
Detective Quantum Efficiency	80%@8 - 12 keV	100%@8 keV, 80%@12 keV, 50%@16 keV
Dynamic Range	32'768 - 131'072	1'048'576
Framing Rate	0.01 - 0.5 Hz	10 - 100 Hz
Pixel Size	0.05 - 0.15 mm	0.172 mm
Read-out Time	1 - 120 s	5 ms
Signal to Noise Ratio	Limited by dark current and noise	Fluorescent background suppression
Point Spread Function	Several pixels	One Pixel

Pilatus 12M for S-SAD phasing

http://www.dectris.com

The use of long wavelengths for anomalous phasing has long been hampered by strong air absorption and large scattering angles. A PILATUS 12M specific solution, built by DECTRIS in close collaboration with the I23 team of Diamond Light Source (DLS), effectively overcomes these limitations. Placing sample and detector in vacuum eliminates air absorption. The semi cylindrical shape of the detector covers a 2-theta range of ±100° and allows the simultaneous collection of low- and high-resolution data.

2000s: Automation

Crystallization / nanodrops

Sample changers / sample holder standard

Automation: Sample changer

Manual handling

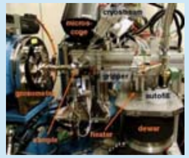

ALS

EMBL

Rigaku

FIP

APS

Higher reliability
Better reproducibility
=> screening, to find the best crystal

Automation
Software

- MxCube
- ISPyB
- EDNA / xdsadp, meXDS, etc.

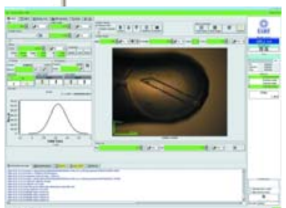

In situ screening / data collection

Diffraction "in the plate"
=> no crystal handling
Great for fragile crystals (larges complexes...), RT, ligand screening

in situ screening & data collection

- SBS micro-plates (sitting/hanging drops)
- SBS high density batch plates
- micro-chips
- high pressure cells

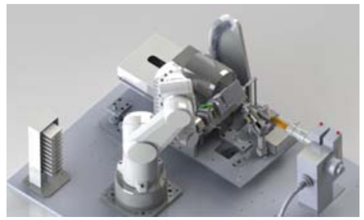

Applications

- rapid crystallization screening
- data collection on fragile crystals, significantly degraded upon freezing
- data collection at room temperature on series of crystals
- automated screening of compounds, fragments, heavy atoms

96-well crystallization plate

1536-well micro-batch plate

FIP-BM30A (ESRF)
CBS (Montpellier)

Bovine enterovirus 2
Crystallization plate screening on I24

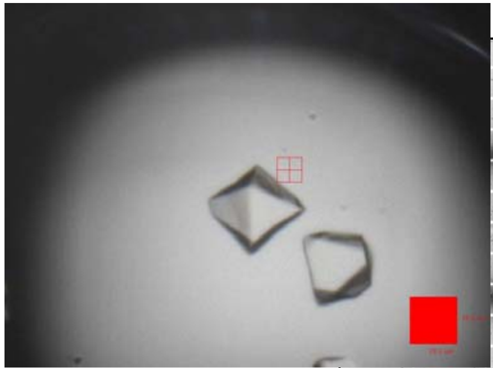
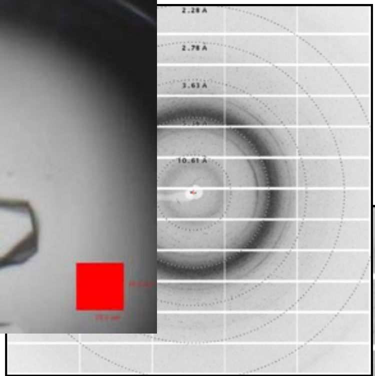
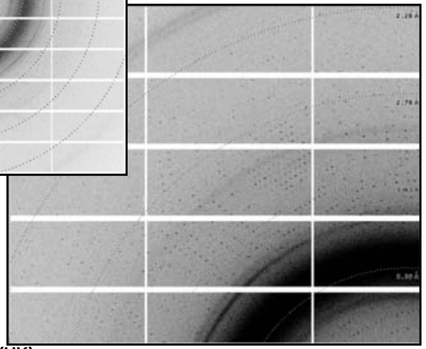
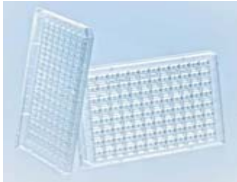

Data collected at DLS, I24
Beam size 20 microns, focus at detector (P6M)
exposure time 0.1 sec, 0.1° oscillation,
detector distance = 480 & 645 mm,
resolution at edge of detector 2.28 & 2.97 Å

E.E. Fry, J.S. Ren, A. Kotecha, T.S. Walter, C. Porta, D.I. Stuart,
The Wellcome Trust Centre for Human Genetics, University of Oxford (UK),
D.J. Rowlands, Institute of Molecular and Cellular Biology, University of Leeds (UK) and
Gwyndaf Evans, Robin Owen, Danny Axford, Jun Ashima, I24, Diamond Light Source (UK)

A new virus structure: Bovine enterovirus 2
Crystallization plate screening on I24 (DLS)

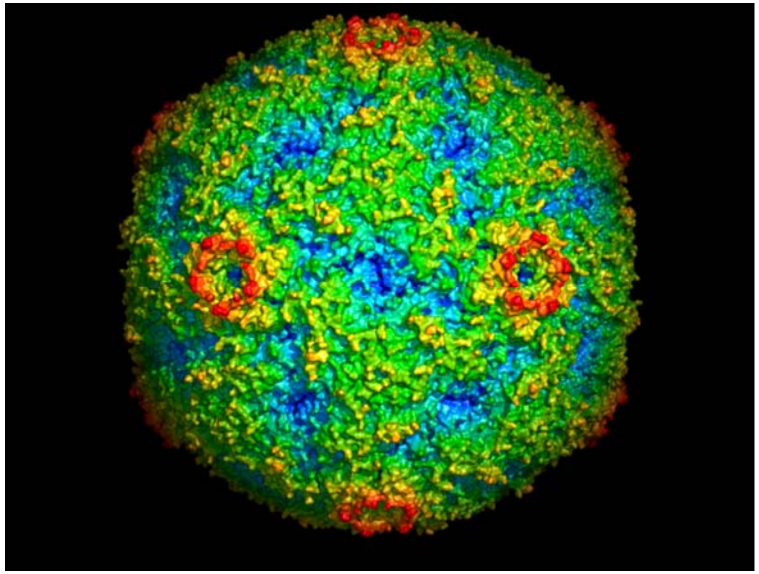

E.E. Fry, J.S. Ren, A. Kotecha, T.S. Walter, C. Porta, D.I. Stuart,
The Wellcome Trust Centre for Human Genetics, University of Oxford (UK),
D.J. Rowlands, Institute of Molecular and Cellular Biology, University of Leeds (UK) and
Gwyndaf Evans, Robin Owen, Danny Axford, Jun Ashima, I24, Diamond Light Source (UK)

2010s: 3rd+/4th generation sources

X-ray sources
Fast SS detectors

Micro/nano crystals

Room temperature / serial data collection

XFELs: 4th generation X-ray sources

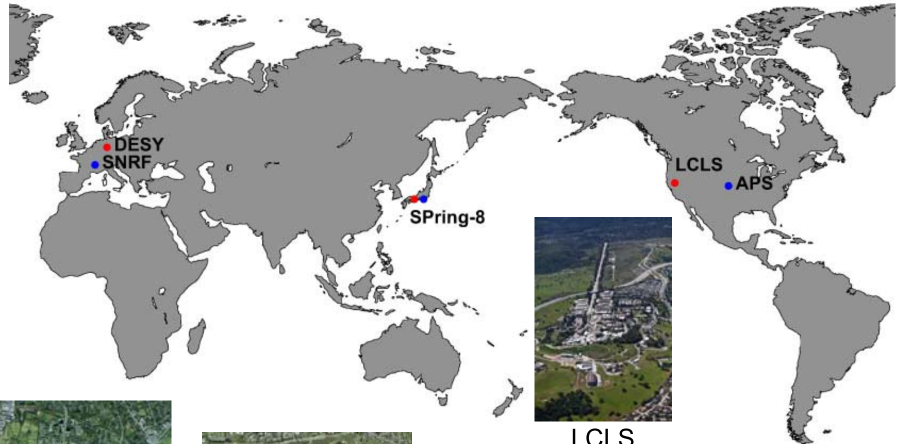

LCLS (Stanford)

European XFEL (Germany)

SwissFEL (Viligen)

SACLA (Japan)

XFEL-O (Argonne)

XFELs: 4th generation X-ray sources

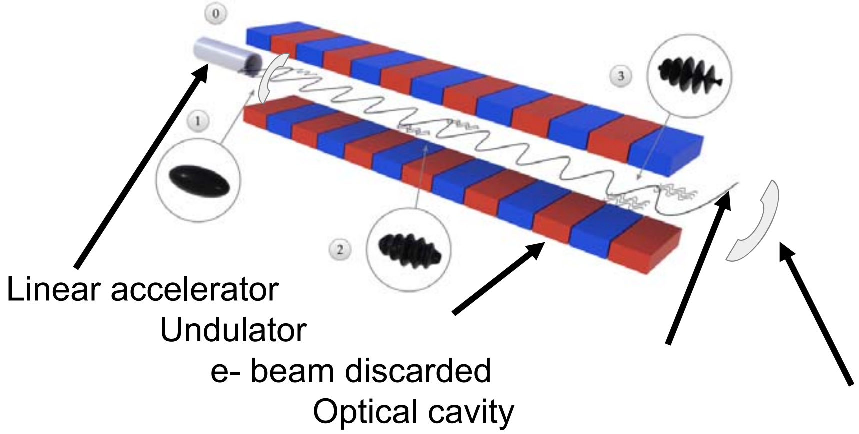

Long undulator => **micro-bunching** of the electron beam
=> **self amplificating spontaneous emission**
e- in undulator field → X-ray beam
e- in X-ray beam field → X-ray beam exponentially
Transverse and longitudinal coherent beam

European XFEL

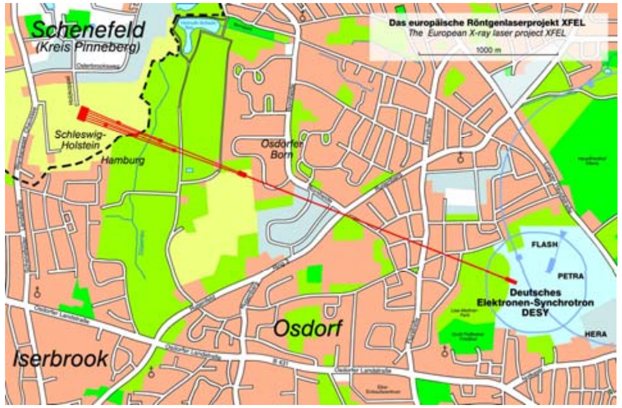

Length: 3,4km

Multi-User Capability

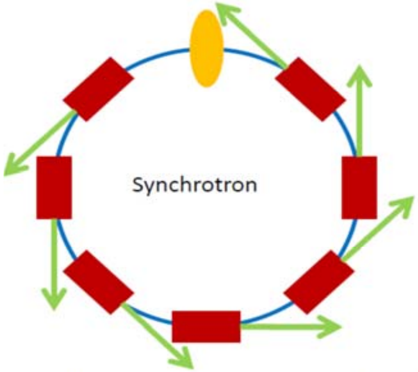

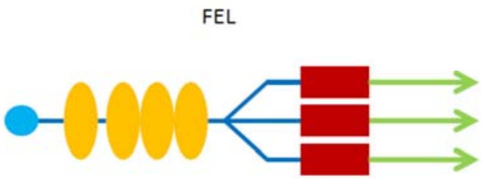

Synchrotron can support many beam lines

Incoherent undulator radiation included in equilibrium beam parameters.

Accelerator cavity restores energy lost to X-rays

FEL interaction increases beam energy spread, cannot re-use beam

Can use fast magnet (kicker) to distribute a multi-bunch beam among multiple undulators

Accelerator magnets cannot change quickly, so need to run all bunches at very similar energy -> adjustable gap undulators for tuning.

37

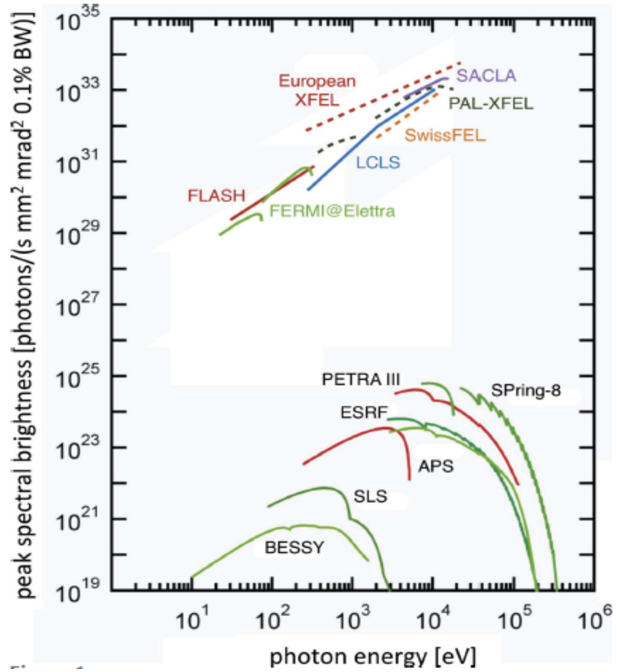

***De novo* protein crystal structure determination from X-ray free-electron laser data**

Thomas R. M. Barends[1], Lutz Foucar[1], Sabine Botha[1], R. Bruce Doak[1,2], Robert L. Shoeman[1], Karol Nass[1], Jason E. Koglin[3], Garth J. Williams[3], Sébastien Boutet[3], Marc Messerschmidt[3] & Ilme Schlichting[1]

244 | NATURE | VOL 505 | 9 JANUARY 2014

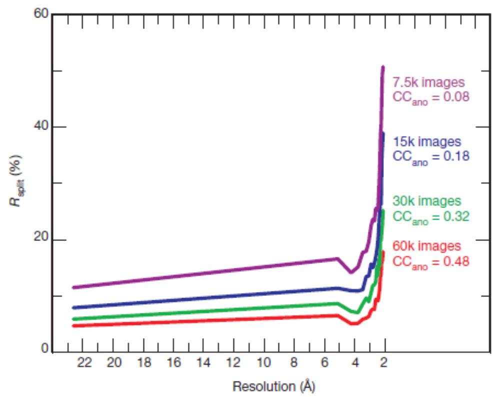

Figure 4 | Data quality as a function of resolution and number of indexed patterns used to derive integrated intensities as shown by R_{split}. The anomalous correlation coefficient CC_{ano} for the whole resolution range is indicated as well.

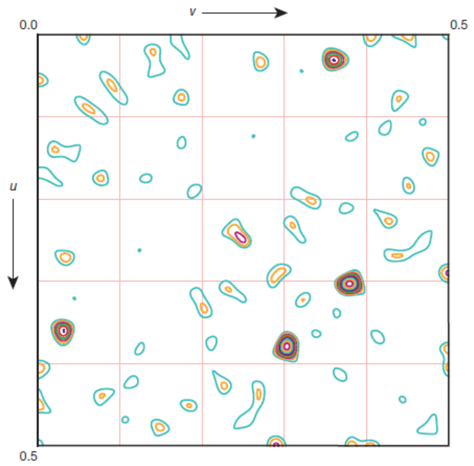

Figure 1 | $w = 0.5$ section of the origin-removed, super-sharpened anomalous difference Patterson map of the SFX lysozyme gadolinium data, using ~60,000 images. Clear peaks are observed from the anomalous scattering of the gadolinium atoms. This figure was prepared using XPREP.

4^{th} generation X-ray sources:
Sample dispensing

Sample destroyed upon exposure to the beam (1 frame /sample)
→ samples to intercept the beam at an high frequency
→ merging of many randomly collected diffraction frames

Crystals in droplets ejected with sonic waves

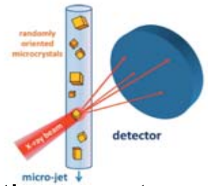

Continuous stream of nano-crystals solution

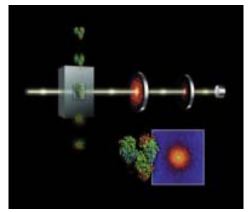

Up to single particules analysis ?

4^{th} generation X-ray sources:
Detectors

Present fast detectors
dead time ~1 msec

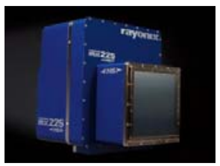

MH-HS (Rayonix)

Pilatus (Dectris)

Starting operation
dead time ~3 usec

Eiger (Dectris)

To come…
3.5 MHz frame rate!

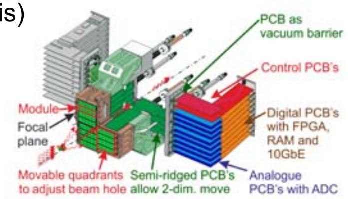

AGIPD (DESY, PSI)
(Allahgholi et al., Journal of Instrumentation, 10 2015)

3 and $3+^{rd}$ generation X-ray sources:
Serial data collection

Convergence between in situ approach on 3^{rd} gen. sources and high rate sample dispensing on X-FELs

A large number of small crystals used to collect partial dataset at room temperature
→multiple crystals on a single support
→clustering and merging data

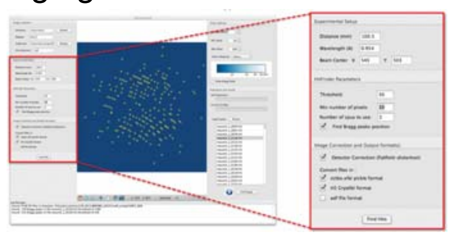

Raster-scanning serial protein crystallography using micro- and nano- focused synchrotron beams. Coquelle et al.. Acta Crystallogr D 71(Pt 5), 2015:1184-96

3+rd generation X-ray sources and sub-micron beams

Project of sub-micron beams, such as VMXu at DLS, ...

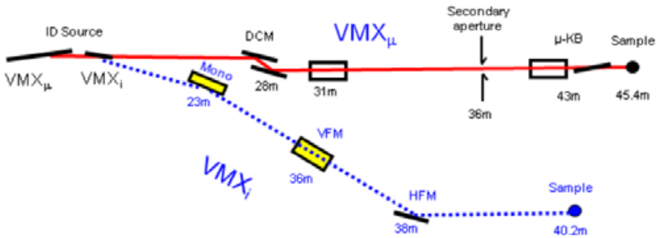

High flux, very small beam size
→ small crystals
→ short exposure
makes possible **complete data collection at RT** before decay

Ultrafast (ms) data collection with ultra-high dose rate
at RT could reduce radiation sensitivity to the one at 100 K
Warkentin et al. (2013) JSR 20, 7
Owen et al. (2012) Acta Cryst D68, 81

The X-ray offer on large facilities

Synchrotron beamlines in France

Synchrotron / Station	Beam	Main equipments	Experiments
ESRF ID23-1	40x30um/0.6-2.5Å	MD2/SC3/Pilatus6M	SAD, MAD
ID23-2	8x6um/0.873Å	MD2/SC3/Mosaic225	single wav.
ID29	10x75um/0.7-2.1Å	MD2/SC3/Pilatus6M	SAD, MAD
ID30A1	100x65um/0.968Å	RoboDiff/Pilatus6M	single wav.
ID30A3	15um/0.984Å	MD2/SC3/Pilatus2M	single wav.
ID30B	20x20um/0.62-2.1Å	MD2/SC3/Pilatus6M	SAD, MAD
BM14	???/0.7-1.8Å	MD2/G-Rob/Mosaic225	in situ/SAD/MAD
BM30A	300um/0.7-1.8Å	MD2/G-Rob/ADSC315	in situ/SAD/MAD
SOLEIL			
Proxima1	100um/0.84-2.5Å	Kappa/CATS/Pilatus6M	SAD, MAD
Proxima2A	5um/0.84-2.5Å	MD2/CATS/Eiger	SAD, MAD

Synchrotron beamlines in Europe

Synchrotron	Station	Beam	Experiments
SLS	PXI-X06SA	10x40um/0.72-2.2Å	SAD/MAD
	PXII-X10SA	50x10um/0.62-2.07Å	SAD/MAD
	PXIII-X06DA	80x45um/0.71-2.07Å	SAD/MAD/in situ
DLS	I02	80x20um/0.5-2.5Å	SAD/MAD
	I03	80x20um/0.5-2.5Å	SAD/MAD/in situ
	I04-1	???/0.92Å	single wav./in situ
	I04	10x5um/0.88-2.07Å	SAD/MAD
	I23	*1.5-4Å*	*sulphur SAD*
	I24	10x10um/0.7-2.0Å	SAD/MAD/in situ
	VMXi / VMXu… (I02)		
BESSY	MX14-1	40-30um/0.8-2.5Å	SAD/MAD
	MX14-2	180x70um/0.8-2.5Å	SAD/MAD
	MX14-3	180x110um/0.91Å	single wav.
PETRAIII	P13	30x20um/0.7-2.7Å	SAD/MAD
	P14	5x5um/0.6-2.1Å	SAD/MAD
MAXII	BLI711	???/0.9-1.5 Å	SAD/MAD
ELETTRA	XRD1	200um/0.6-3.15Å	SAD/MAD
ALBA	BL13-XALOC	50x10um/0.6-2.4Å	SAD/MAD

Access to

FIP-BM30A, ID23, ID29, ID30-MASSIF (ESRF): ESRF call for proposal

FIP-BM30A, Proxima1, Proxima2: SOLEIL call for proposal

In the future:

European XFEL

ESS